

Effects of Deposition Method of PECVD Silicon Nitride as MIM Capacitor Dielectric for GaAs HBT Technology

Jiro Yota

GaAs Technology, Skyworks Solutions, Inc.
2427 W. Hillcrest Drive, Newbury Park, CA 91320, USA
jiro.yota@skyworksinc.com

Thin silicon nitride (Si_3N_4) films deposited using plasma-enhanced chemical deposition (PECVD) method have been used as metal-insulator-metal (MIM) capacitor dielectric for GaAs hetero-junction bipolar transistor (HBT) technology. The characteristics of the films, which were deposited at 300°C , were found to be dependent on how the PECVD film was deposited. A silicon nitride film deposited as a multi-layer-layer film has different properties compared to a film deposited under the same processing conditions as a single layer film. When used as MIM capacitor dielectric, the multi-layer Si_3N_4 film is shown to have significantly superior and higher dielectric breakdown voltage and lower leakage current characteristics, as compared to the single layer film, while the capacitance density is found to be similar. Additionally, the multi-layer Si_3N_4 film is shown to have lower compressive stress and lower refractive index, indicating that the characteristics of the film are influenced by the additional interfaces present in a multi-layer film.

Introduction

Due to the increasing demand for capacity and revenue, the die size in semiconductor wafer manufacturing must be reduced. One method to reduce the die size of circuit designs is to increase the capacitance density of metal-insulator-metal (MIM) capacitor device, which is a key passive component in GaAs-based technologies, including hetero-junction bipolar transistor (HBT) technology [1-10]. The capacitance density of capacitors can be increased by simply reducing the thickness of the capacitor dielectric or insulator. However, reducing this dielectric thickness will typically also reduce the breakdown voltage and increase the leakage current of the capacitor, and thereby, degrading the performance of the device. Therefore, it is imperative that the dielectric film is well optimized, resulting in a film with desired thickness, and electrical, physical, and chemical characteristics. The electrical characteristics of a MIM capacitor dielectric in GaAs HBT technology typically should include high capacitance density, high dielectric breakdown voltage, and low leakage current, and the capacitor needs to meet and satisfy the performance and reliability requirements of the devices and circuits [2,4,8,11].

In semiconductor technology, there are multiple materials that can be used as MIM capacitor dielectric. They include silicon nitride (Si_3N_4), silicon oxynitride, and

Symposium on Silicon Nitride, Silicon Dioxide, and Emerging Dielectrics of the 2011 Electrochemical Society (ECS) Meeting, May 1-6, 2011, Montreal, Canada

various higher dielectric constant materials, such as tantalum oxide, hafnium oxide, aluminum oxide, niobium oxide, strontium oxide, and many others, including composite oxides [8,12-22]. The silicon nitride and silicon oxynitride as capacitor dielectric is typically deposited using plasma-enhanced chemical vapor deposition (PECVD) [3,4,7,8,23], while the higher dielectric constant materials are typically deposited using sputtering, atomic layer deposition (ALD), or other deposition methods [17,19,20]. The most common dielectric material used as the insulator or dielectric for MIM capacitors in GaAs HBT technology is PECVD silicon nitride, due to its good electrical characteristics, including relatively high dielectric constant, high dielectric breakdown voltage, and low leakage current, and due to its compatibility with GaAs processing [1-4,7,8]. The application of PECVD Si_3N_4 film, which can be deposited at temperature of 300°C or lower, will minimize device degradation that may occur when GaAs devices are exposed to higher processing temperatures [4,8,10,24-26].

A PECVD silicon nitride film can be deposited as a single layer film or as a multi-layer film, depending on the tool and process configuration. A single layer film will only have two surfaces, one on each side of the film, while a multi-layer film, in addition to the two surfaces, will have multiple interfaces separating the layers, and which is determined by how many layers are deposited. Previous studies on PECVD multi-layer films, including silicon oxynitride, carbon-doped silicon dioxide, and silicon nitride, show that the elemental concentration at the surfaces and interfaces are different compared to the concentration within the bulk of the film or within each layer [27-32]. The different elemental concentration at surfaces and the interfaces of the film is most likely caused by the deposition method [27-32]. During a silicon nitride deposition process, typically, reactant gases are flowed into the PECVD deposition chamber, before the RF power is turned on and any of the main reactions occur. In this initial stage, even though the RF power is still not on, some reactions or deposition can already occur on the wafer substrate surface. These reactions will result in a film with different elemental concentration at the surfaces and interfaces within the film that is different compared to the concentration of the film when the RF power is on during the deposition and the process condition is stable. It has been shown in previous studies that multi-layer PECVD films have different glass transition temperature [28], optical properties [29], and dielectric breakdown strength [30,31], compared to single layer films. Additionally, a multi-layer PECVD film is known to have no or minimal pinholes within the film, as compared to single layer film. This is due to the fact that during a multi-layer deposition, any pinholes that may be present or form in a particular layer of the film, will be covered by the overlying and subsequent layers. This lack of pinholes has been shown to improve the reliability of devices utilizing the multi-layer film and make the film to be more suitable for various applications, such as capacitor dielectric, pre-metal dielectric, surface passivation, final passivation, and interlevel dielectric [4,8,24,32-35].

In this study, we have deposited and characterized various PECVD silicon nitride films for MIM capacitor dielectric applications in GaAs HBT technology. We have compared the properties of single layer and multi-layer films, deposited under the same processing conditions. Physical and optical characterization was performed by studying the stress and refractive index of these silicon nitride films. Furthermore, the conformality and surface roughness of the PECVD Si_3N_4 film were also evaluated, in addition to the chemical bonds present in the film. Electrical characterization was

performed by studying the capacitance density, breakdown voltage, and current-voltage (I-V) characteristics of the silicon nitride film, when used as a capacitor dielectric of a metal-insulator-metal capacitor.

Experimental

The deposition of silicon nitride (Si_3N_4) films used as the capacitor insulator or dielectric in a metal-insulator-metal (MIM) capacitor was performed using plasma-enhanced chemical vapor deposition (PECVD) method. The films, ranging in thickness from 500 Å to 700 Å, were deposited on both 4-inch GaAs bare and device wafers, and were processed using GaAs hetero-junction bipolar transistor (HBT) technology. The devices on the wafers include HBT devices and metal-insulator-metal (MIM) capacitors. The bottom conductor (Metal 1) of the MIM capacitor consists of 1 μm Ti/Au/Ti metal stack, while the top conductor (Metal 2) consists of 2 μm Ti/Au/Ti stack. Two different areas of MIM capacitor structure were investigated in this study, which are 250 μm^2 and 23,000 μm^2 .

The chemical vapor deposition system used to deposit the PECVD silicon nitride films is a Novellus Concept One (C-1) multi-station sequential deposition system [4,8]. This system allows both single layer and multi-layer films to be deposited on the wafer substrates. There are seven deposition stations in the process chamber. Each deposition station consists of a single wafer pedestal and a gas shower head. All wafers in the chamber are placed on a resistively heated pedestal or heater block which results in quick and uniform wafer heating. Process gases are introduced into and distributed to each of the seven showerheads for the deposition. All the process gases and process by-products for the entire reactor are evacuated through a single vacuum line at the center of this PECVD process chamber.

Single layer deposition is performed by placing one wafer on each of the seven stations, and then by depositing the total desired thickness at the same time on all seven wafers. For a multi-layer deposition, wafers are sequentially processed through each deposition station where they receive one-seventh of the total deposition thickness. Therefore, the resulting thickness is the same for both the single layer film and the multi-layer film, when the total deposition time is the same. Figure 1 shows a diagram comparing the silicon nitride film deposited using a single layer or multi-layer method. As can be seen in the figure, the single layer film has one surface on each side, while the multi-layer film, deposited on seven stations and resulting in seven layers, has six interfaces, in addition to the two surfaces.

In this study, the PECVD process condition of the Si_3N_4 is kept the same for both single and multi-layer films, including the same gas flow rates, deposition pressure, temperature, and the RF power. The deposition temperature is 300°C. The RF power used is a combination of both high frequency (HF) and low frequency (LF) power. The gases used are silane (SiH_4), ammonia (NH_3), and nitrogen (N_2). Both silane and ammonia are the reactant gases, while the nitrogen is used as a diluents gas. The NH_3 gas is flown continuously during the process to maintain chamber pressure, while the SiH_4 and N_2 gases are flown during the deposition process only. The sequence of events,

Symposium on Silicon Nitride, Silicon Dioxide, and Emerging Dielectrics of the 2011 Electrochemical Society (ECS) Meeting, May 1-6, 2011, Montreal, Canada

including the time when the gases are introduced into the deposition chamber and the time when the RF power is turned on in this study, is shown in Figure 2. As can be seen, in the initial stages of the process, the SiH_4 and N_2 are introduced into the process chamber, before the RF power is turned on and the deposition occurs. At the end of the deposition process, the SiH_4 and N_2 stop flowing, followed by the RF power being turned off. Since the process conditions are the same for both single layer and multi-layer films, the deposition rate of both films deposited is also the same. The only difference between these two deposition methods is the deposition time in each station. As discussed before, the deposition time of the multi-layer film per station is one-seventh of that of a single layer film. However, the total deposition time and the resulting thickness for both films are the same.

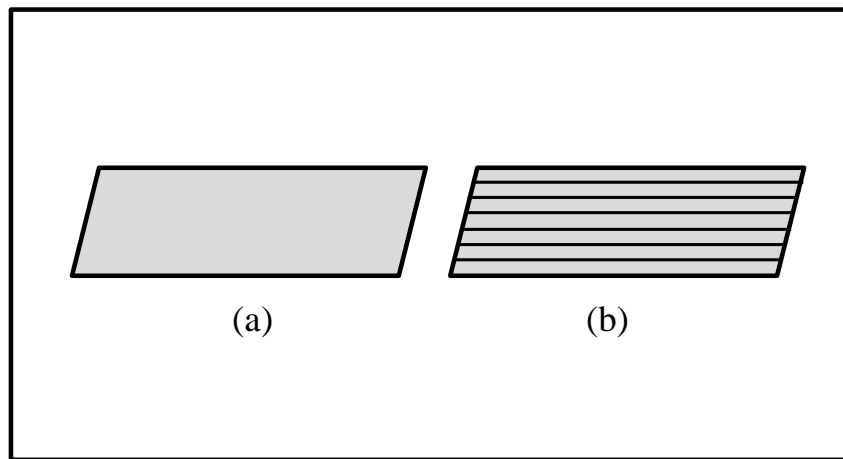


Figure 1. Comparison between (a) single layer and (b) multi-layer PECVD film deposited in this study.

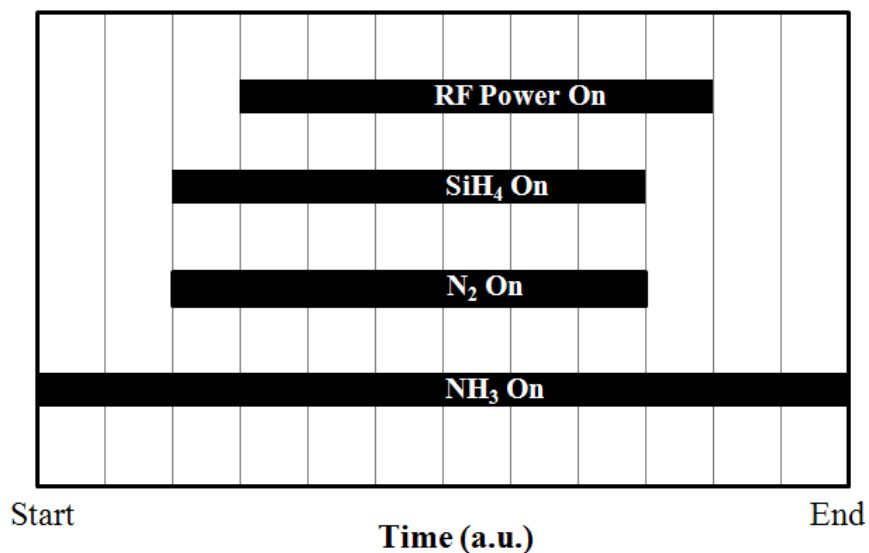


Figure 2. The sequence of events during the deposition of PECVD silicon nitride film in this study.

Both the thickness and refractive index of the silicon nitride films were measured using a Rudolph FE-VII ellipsometer, while the stress was obtained using a Frontier FSM 8800 system. Fourier Transform Infrared (FTIR) analysis was performed using a Nicolet Magan 550 at 4 cm^{-1} resolution. The FTIR analysis was performed on 600 \AA PECVD Si_3N_4 films deposited on bare GaAs test wafers. Current-Voltage (I-V) and capacitance measurements were obtained using both a manual probe station (Agilent B1500A semiconductor device analyzer) and an automatic parametric tester (Agilent 4284A Precision LCR meter). Ramped voltage measurements were performed with a ramp rate of 1 V/sec , while monitoring the current until breakdown occurs. Focused-Ion Beam/Scanning Electron Microscopy (FIB/SEM) analysis was performed using a FEI 820 dual beam system.

Results and Discussion

Stress and Refractive Index

Figure 3 shows the stress of 600 \AA silicon nitride films deposited using two different methods of single layer and multi-layer deposition processes. As can be seen, the single layer film has a compressive stress of -118 MPa , while the multi-layer film has a lower compressive stress of -72 MPa . Figure 4 shows the refractive index of a single layer 600 \AA Si_3N_4 film and multi-layer films with different thicknesses, ranging from 500 \AA to 700 \AA . It can be observed that for this range of thicknesses investigated, there is no significant difference in refractive index for the multi-layer films, with refractive index ranging from 1.884 to 1.889 , while the 600 \AA single layer silicon nitride film has a much higher refractive index of 1.918 . The lower refractive index and compressive stress of the multi-layer film most likely are caused by the presence of interfaces within the film, which results in a silicon nitride film containing lower concentration of Si and higher concentration of N.

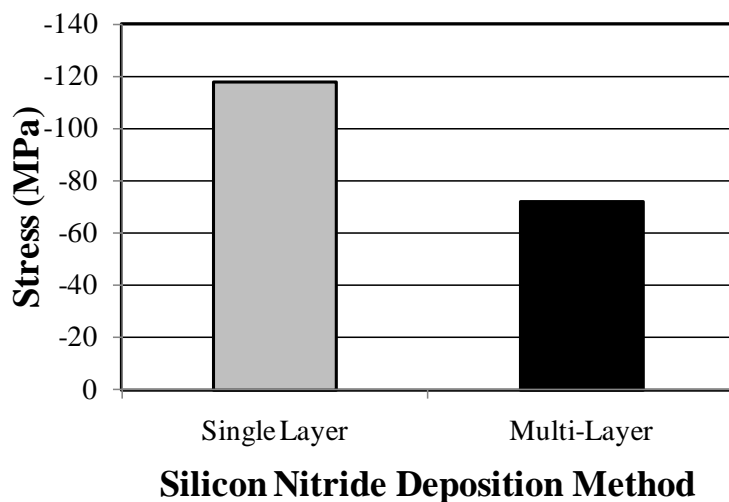


Figure 3. The compressive stress of 600 \AA PECVD silicon nitride deposited using single layer and multi-layer deposition methods.

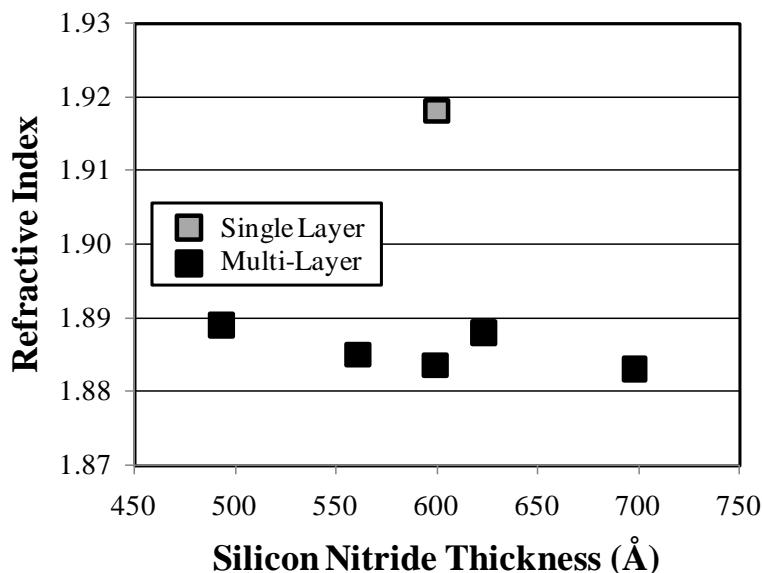


Figure 4. The refractive index of the PECVD silicon nitride deposited using single layer and multi-layer deposition methods.

FTIR Analysis

Fourier Transform Infrared (FTIR) analysis was performed to investigate the nature of chemical bonds present in the PECVD silicon nitride films, and to evaluate whether there are any significant differences that can be detected or observed between the deposited single layer and multi-layer films. Figure 5 shows the infrared spectra of these two types of Si_3N_4 films. It can be seen that the infrared absorbance peaks that are present in both spectra include those of the Si-N stretching mode (860 cm^{-1}), the N-H bending mode (1160 cm^{-1}), the N-H stretching mode (3340 cm^{-1}) and the Si-H stretching bonds (2200 cm^{-1}) [4,32,33]. These spectra show that the two silicon nitride films contain a significant amount of hydrogen, as indicated by the presence of the absorbance peaks of Si-H and N-H bonds. These results are typical for PECVD Si_3N_4 films and are consistent with previous studies [4,8,32,33]. There may be some slight difference in some of these infrared peaks present in the spectra of these two films. However, the differences, if any, cannot be detected and observed using this FTIR analysis.

Electrical Characterization

Electrical characterization of the two types of Si_3N_4 film, when used as capacitor dielectric of an MIM capacitor, was performed by evaluating the capacitance, breakdown voltage, and current-voltage (I-V) characteristics. Figure 6 shows the capacitance density data of a capacitor using a dielectric of a single layer 600 Å silicon nitride film, and of multi-layer silicon nitride films with different thicknesses, ranging from 500 Å to 700 Å. As can be seen, the capacitance density obtained is about $0.942\text{ fF}/\mu\text{m}^2$, and there is no

significant difference observed between the 600 Å single layer and the 600 Å thick multi-layer Si_3N_4 capacitor dielectric films. Furthermore, as expected, the data also shows that the capacitance density is reduced as the silicon nitride film thickness is increased. Figure 7 shows the capacitance of MIM capacitors with a small area of $250 \mu\text{m}^2$ and a much larger area of $23,000 \mu\text{m}^2$, using these two types of 600 Å Si_3N_4 films. As shown, Figure 7 shows that there is no significant difference in capacitance between these two films for both capacitor areas. All the above data indicate that the capacitance characteristics of these films are very similar.

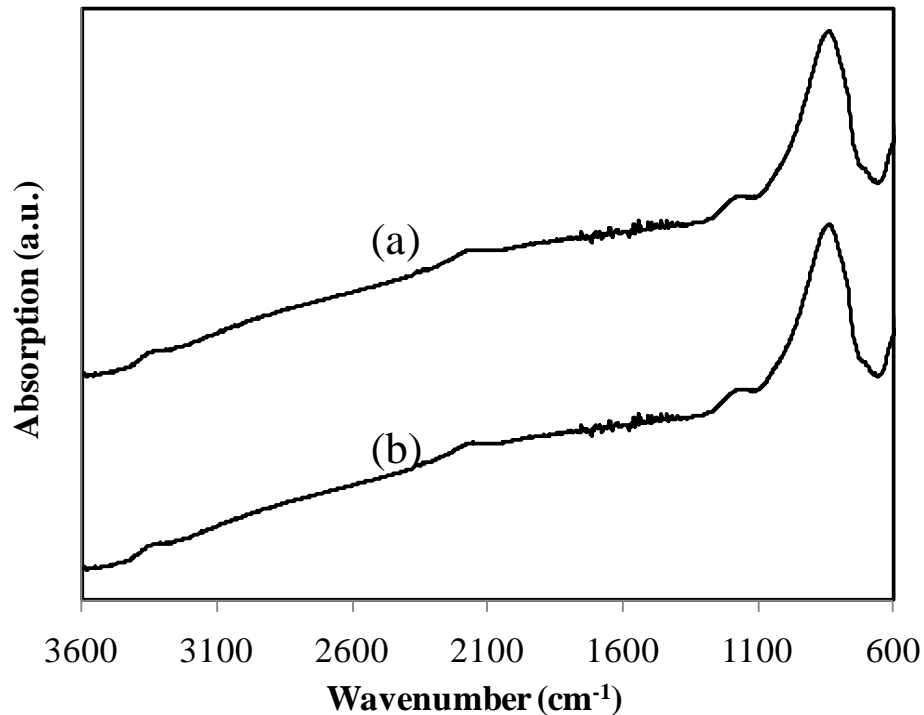


Figure 5. The infrared spectra of the PECVD silicon nitride deposited using (a) single layer and (b) multi-layer deposition methods.

Figure 8 shows the current voltage (I-V) curves obtained from MIM capacitors using a capacitor dielectric of a single layer 600 Å PECVD silicon nitride film, and of multi-layer silicon nitride films with different thicknesses. As expected, the leakage current increases when the capacitor dielectric film thickness is decreased for the Si_3N_4 films deposited using the same method. However, as can be seen, the capacitor with the single layer 600 Å Si_3N_4 film has significantly higher leakage current, as compared to the capacitor with multi-layer films, irrespective of the thickness in the range of 500 Å to 700 Å. The observed results indicate that the multi-layer film has superior and lower leakage current characteristics than the single layer. The multi-layer silicon nitride films also show superior and higher breakdown voltage characteristics. Figure 9 shows the dielectric breakdown voltage of the 600 Å Si_3N_4 deposited as a multi-layer film is 63 V, which is 7.23% higher than that of the 600 Å deposited as a single layer film, which

breakdown voltage is 58.75 V. Furthermore, Figure 9 also shows that the breakdown voltage of multi-layer silicon nitride films increases with increasing film thickness.

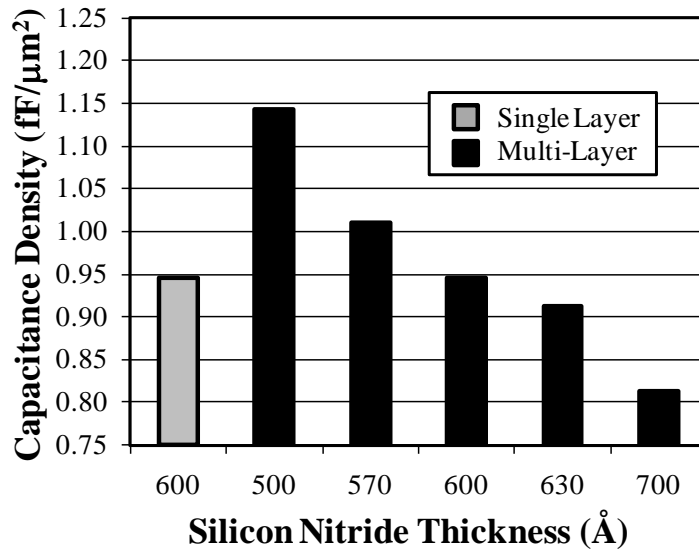


Figure 6. The capacitance density of MIM capacitor using the PECVD silicon nitride as capacitor dielectric with different thicknesses, deposited using single layer and multi-layer deposition methods.

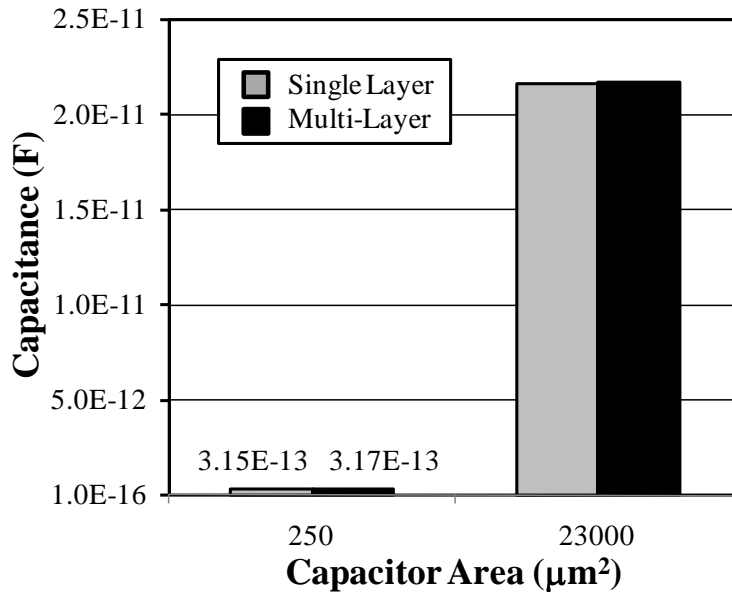


Figure 7. The capacitance density of MIM capacitor of different areas, using 600 Å PECVD silicon nitride film as capacitor dielectric, deposited using single layer and multi-layer deposition methods.

The MIM capacitor electrical characterization data show that the Si_3N_4 deposited as a multi-layer film is significantly superior in electrical characteristics than the single layer film. For the same thickness, both types of film yield similar capacitances, while at the same time, the multi-layer Si_3N_4 film shows much lower leakage current and higher dielectric breakdown voltage. These superior characteristics may be attributed to the presence of multiple interfaces with differing elemental concentrations and the presence of minimal pinholes, if any, in a multi-layer film. This is especially important, if the underlying metal or electrode used in the MIM capacitor has a rough surface, which is typical for evaporated metal usually used in the GaAs processing [4,8]. During this multi-layer PECVD silicon nitride film deposition, each layer that is deposited will cover conformally and eliminate or reduce any surface roughness and sharp features of the underlying metal. All these make this multi-layer dielectric film to be very much suitable for MIM capacitor application in GaAs HBT technology [4,8].

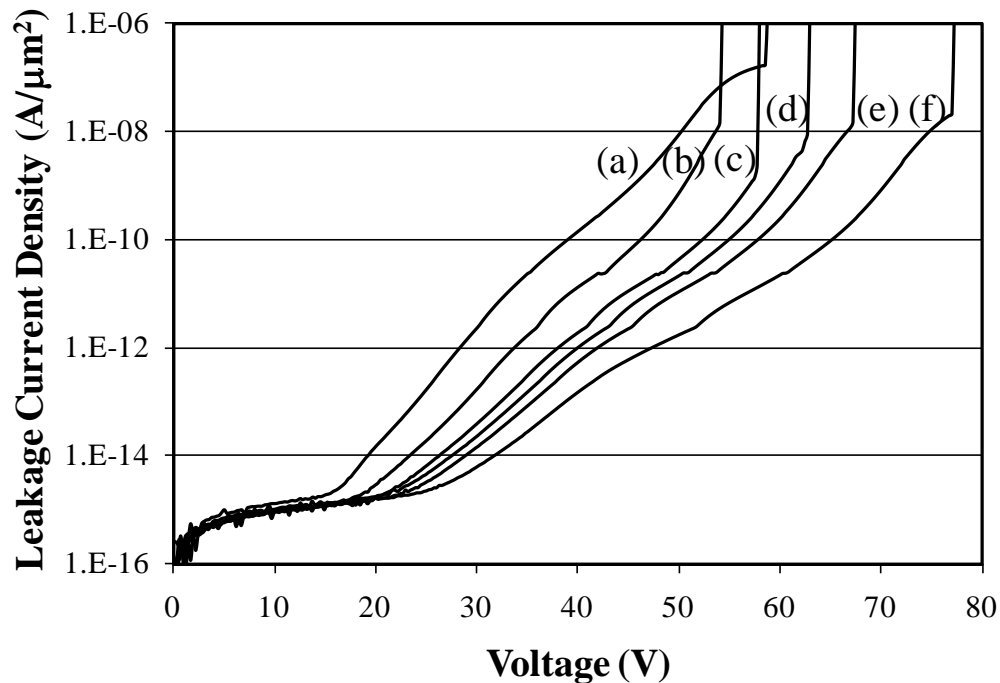


Figure 8. The current-voltage (I-V) curves of MIM capacitor, with (a) 600 Å single layer, and (b) 500 Å, (c) 570 Å, (d) 600 Å, (e) 630 Å, and (f) 700 Å multi-layer PECVD silicon nitride capacitor dielectric.

FIB/SEM Analysis

Figure 10 shows the Focused-Ion Beam/Scanning Electron Microscopy (FIB/SEM) images of an MIM capacitor with 600 Å multi-layer PECVD Si_3N_4 as capacitor dielectric, and the hetero-junction bipolar transistor (HBT) with the emitter, base, and collector, on a GaAs wafer manufactured using GaAs HBT technology. As shown, the PECVD silicon nitride film is conformal and has excellent step coverage over the rough underlying Metal 1 surface, and in fact, reduces this metal surface roughness. This good conformality is critical in order to reduce increased electric field and fringe capacitance due to the sharp features and non-uniformity of the underlying metal

conductor surface [4,8]. The images in Figure 10 show that the multi-layer Si_3N_4 is very suitable and excellent for MIM capacitor dielectric application in GaAs HBT technology.

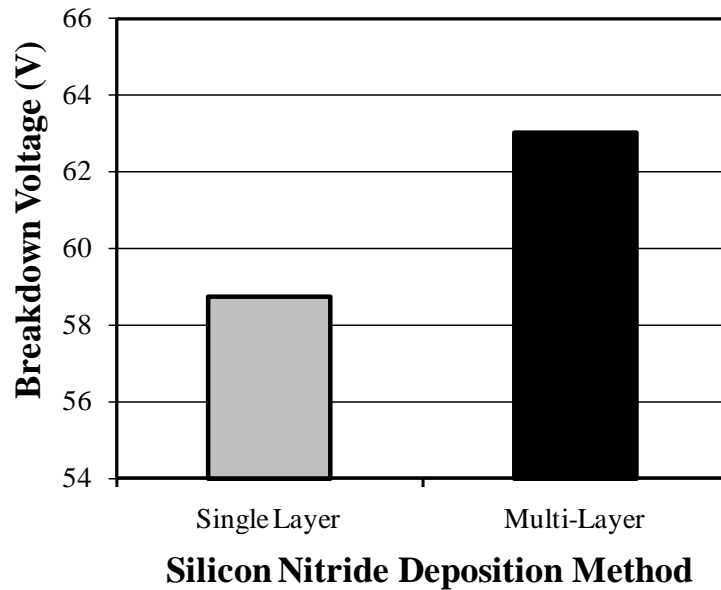


Figure 9. The dielectric breakdown voltage of MIM capacitor using 600 Å PECVD silicon nitride film as capacitor dielectric, deposited using single layer and multi-layer deposition methods.

Conclusions

We have evaluated the use of thin silicon nitride (Si_3N_4) films deposited using plasma-enhanced chemical deposition (PECVD) method as metal-insulator-metal (MIM) capacitor dielectric. The film characteristics were found to be dependent on the deposition method, including whether the film is deposited as a single layer or multi-layer film. The multi-layer Si_3N_4 film is shown to have lower compressive stress and lower refractive index, compared to the single layer film. FTIR data show that there is no significant difference in chemical bonds present in the film between the two types of silicon nitride. Electrical characterization of MIM capacitor shows that there is no significant difference in the capacitance density obtained when a single layer silicon nitride or a multi-layer silicon nitride is used as the capacitor dielectric. However, the multi-layer silicon nitride film is shown to have significantly superior and higher dielectric breakdown voltage and lower leakage current characteristics, as compared to the single layer film, making it very suitable for capacitor dielectric application in GaAs HBT technology.

Acknowledgments

The author would like to acknowledge Ravi Ramanathan, Jose Arreaga, Bruce Darley, Daniel Weaver, David Tuunanen, and Mike Sun of Skyworks Solutions, Inc. for their help in this study.

Symposium on Silicon Nitride, Silicon Dioxide, and Emerging Dielectrics of the 2011 Electrochemical Society (ECS) Meeting, May 1-6, 2011, Montreal, Canada

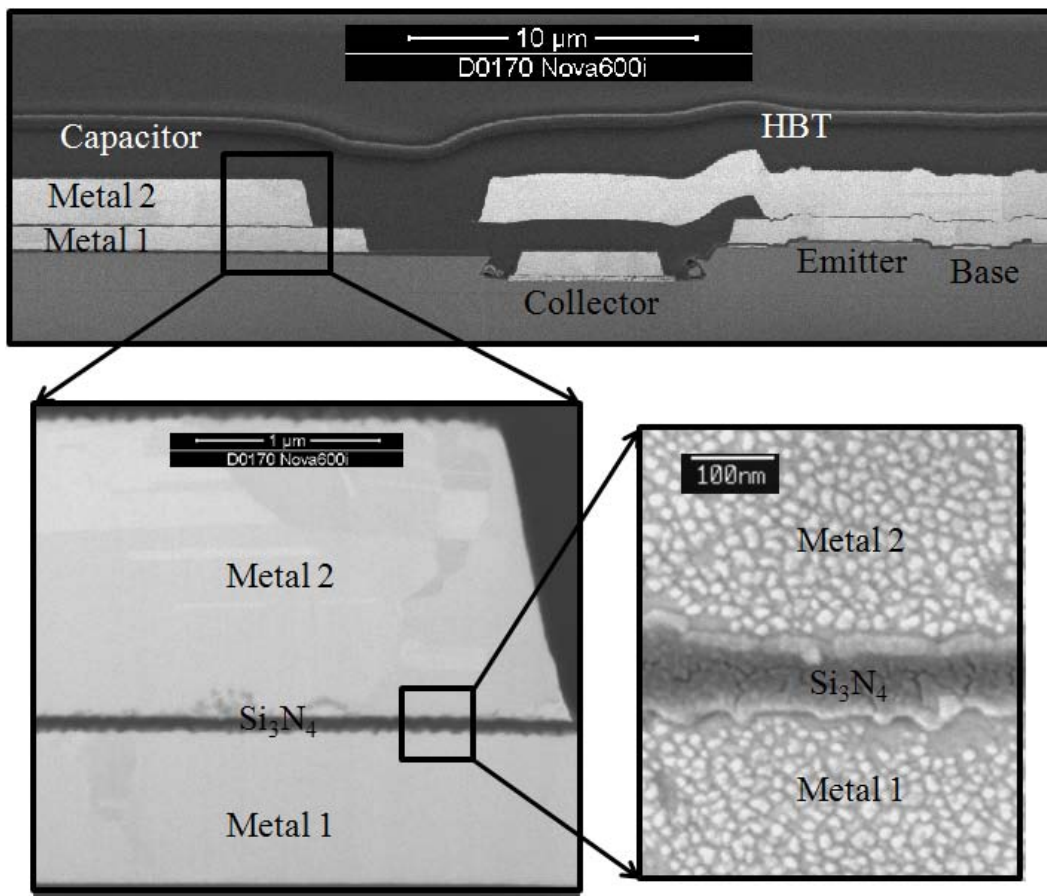


Figure 10. X-Section FIB images of a metal-insulator-metal (MIM) capacitor with 600 Å multi-layer PECVD silicon nitride as capacitor dielectric and hetero-junction bipolar transistor (HBT) on wafers manufactured using GaAs HBT technology.

References

1. C. Whitman and M. Meeder, in *Reliability of Compound Semiconductors Workshop*, pp. 91-102 (2004).
2. J. Scarpulla, E.D. Ahlers, D.C. Eng, D.L. Leung, S.R. Olson, and C.S. Wu, in *GaAs Reliability Workshop*, pp. 92-105 (1998).
3. G. Dandrova, J.M. Beall, and K.D. Decker, *ECS Trans.*, **6** (3), 397 (2007).
4. J. Yota, R. Ramanathan, J. Arreaga, P. Dai, C. Cismaru, R. Burton, P. Bal, and L. Rushing, in *2003 GaAs MANTECH Tech. Digest*, pp. 65-68 (2003).
5. A. Muller, S. Simion, M. Dragoman, S. Iordanescu, I. Petrini, C. Anton, D. Vasilache, V. Avramescu, A. Coraci, and F. Craciunoiu, in *Proc. International Semiconductor Conference*, pp. 185-188 (1996).
6. C. Nevers, A.T. Ping, T. Rivers, S. Varma, F. Pool, M. Minkoff, E. Etzkorn, and O. Berger, in *2009 CS MANTECH Tech. Digest*, pp. 117-120 (2009).
7. B.N. De and M. Shokrani, in *2005 CS MANTECH Tech. Digest*, pp. 145-148 (2005).
8. J. Yota, R. Ramanathan, K. Kwok, J. Arreaga, T. Ko, and H. Shao, in *Proc. 2005 Electrochemical Society Meeting: State-of-the-Art-Program on Compound Symposium on Silicon Nitride, Silicon Dioxide, and Emerging Dielectrics of the 2011 Electrochemical Society (ECS) Meeting, May 1-6, 2011, Montreal, Canada*

- Semiconductors (SOTAPOCS)*, PV 2005-04, pp. 315, The Electrochemical Society Proceeding Series, Pennington, NJ (2005).
9. T. Kagiya, Y. Tosaka, R. Yamabi, and H. Yano, in *2007 CS MANTECH Tech. Digest*, pp. 51-54 (2007).
 10. R. Williams, *Modern GaAs Processing Methods*, Artech House, Boston (1990).
 11. B. Yeats, *IEEE Trans. Electron. Dev.*, **45** (4), 939 (1998).
 12. A.S. Zoolfakar and H. Hasim, in *Proc. IEEE International Conference on Semiconductor Electronics (ICSE)*, pp. 445-449 (2008).
 13. H. Sanchez, *et al.*, in *Proc. International Interconnect Technology Conference (IITC)*, pp. 84-89 (2007).
 14. N. Inoue, H. Ohtake, I. Kume, N. Furutake, T. Onodera, S. Saito, A. Tanabe, M. Tagami, M. Tada, and Y. Hayashi, in *Proc. International Interconnect Technology Conference (IETC)*, pp. 63-65 (2006).
 15. S.J. Kim, B.J. Cho, M.B. Yu, M.F. Li; Y.Z. Xiong, C.X. Zhu, A. Chin, and D.L. Kwong, *IEEE Electron. Dev. Lett.*, **26**, 625 (2005).
 16. K.C. Chiang, C.H. Lai, A. Chin, H.L. Kao, S.P. McAlister, and C.C. Chi, in *Microwave Symposium Digest*, pp. 287-290 (2005).
 17. H. Hang, *et al.*, in *Proc. IEEE International Electron Devices Meeting (IEDM)*, pp. 379-382 (2003).
 18. T.T. Vo, T. Lacrevez, B. Flechet, A. Farcy, Y. Morand, S. Blonkowski, J. Torres, and E. Defay, in *Proc. Asia-Pacific Microwave Conference*, pp. 1-4 (2007).
 19. N. Menou, *et al.*, in *Proc. IEEE International Electron Devices Meeting (IEDM)*, pp. 1-4 (2008).
 20. N.A. Safford, R. Katamreddy, L. Guerin, B. Feist, C. Dussarat, V. Pallem, C. Weiland, and R. Opila, *ECS Trans.*, **19** (2), 525 (2009).
 21. C. Dubourdieu, O. Salicio, S. Lhostis, L. Auvray, Y. Rozier, F. Ducroquet, and S. Daniele, *ECS Trans.*, **19** (2), 669 (2009).
 22. J. Robertson, *ECS Trans.*, **19** (2), 579 (2009).
 23. M. Maeda, E. Yamamoto, S. Ohfuji, and M. Itsumi, *J. Vac. Sci. & Technol. B*, **17**, 201 (2009).
 24. J. Yota, *J. Electrochem. Soc.*, **156**, G173 (2009).
 25. W. Liu, *Handbook of III-V Heterojunction Bipolar Transistors*, New York, John Wiley (1998).
 26. J. Yota, H. Ly, R. Ramanathan, M. Sun, D. Barone, T. Nguyen, K. Katoh, M. Ohe, R. L. Hubbard and K. Hicks, *IEEE Trans. Semicond. Manuf.*, **20**, 323 (2007).
 27. A.A. Saleh, J.B. Rothman, J.F. Kirchoff, J. Yota, and C. Nguyen, *Thin Solid Films*, **355/356**, 363 (1999).
 28. H. Zhou, H.K. Kim, F.G. Shi, B. Zhao, and J. Yota, *Microelectron. J.*, **33**, 221 (2002).
 29. H. Zhou, H.K. Kim, F.G. Shi, B. Zhao, and J. Yota, *Microelectron. J.*, **33**, 999 (2002).
 30. H. Zhou, F.G. Shi, B. Zhao, and J. Yota, *Microelectron. J.*, **35**, 571 (2004).
 31. H. Zhou, F.G. Shi, B. Zhao, and J. Yota, *Appl. Phys. A*, **81**, 767 (2005).
 32. J. Yota, J. Hander, and A.A. Saleh, *J. Vac. Sci. Technol. A*, **18** (2), 372 (2000).
 33. S. Wolf and R.N. Tauber, *Silicon Processing for the VLSI Era Volume 1 - Process Technology*, Lattice Press, Sunset Beach (1986).
 34. S.K. Gandhi, *VLSI Fabrication Principles, Silicon and Gallium Arsenide*, New York, John Wiley (1983).
 35. J. Yota, *et al.*, in *Proc. 4th Inter. Dielectrics ULSI Multilevel Interconnect. Conf. (DUMIC)*, pp. 185-192 (1998).